An Optimal Flexible Partitioning of Smart Distribution System Considering Electrical and Gas Infrastructure

Sobhan Dorahaki
Department of Electrical Engineering, Shahid Bahonar University
Kerman-Iran
Sobhandorahaki@gmail .com

Masoud Rashidinejad
Department of Electrical Engineering, Shahid Bahonar University
Kerman-Iran
mrashidi@uk.ac.ir

Hossein Farahmand
Department of Electric Power Engineering, Norwegian University of Science and Technology,
Trondheim, Norway
Hossein.Farahmand@ ntnu.no

Mojgan MollahassaniPour
Faculty of Electrical and Computer Engineering,
University of Sistan and Baluchestan Zahedan-Iran
m.mollahassani@ece.usb.ac.ir

Mahdi Pourakbari-Kasmaei
Department of Electrical Engineering and Automation, Aalto University, Maarintie 8, 02150
Espoo, Finland
mahdi.pourakbari@aalto.fi

João P. S. Catalão
Faculty of Engineering of the University of Porto and
INESC TEC,
Porto, Portugal
catalao@fe.up.pt

2021 IEEE Madrid PowerTech | 978-1-6654-3597-0/21/$31.00 ©2021 IEEE | DOI: 10.1109/PowerTech46648.2021.9494956

***Abstract*—The resilient smart distribution system is intended to cope with low probability, high-risk extreme events, including extreme natural disasters. In this regard, the flexible partitioning distribution system into supply-sufficient microgrids can be considered an interesting subject. This paper introduces a novel technique for partitioning a smart distribution system into supply-sufficient microgrids. In the presented model, the impact of demand response programs and energy storage has been considered in the proposed framework. Furthermore, besides the electricity aspects, the effects of gas network infrastructure on flexible portioning are also investigated to improve system resiliency facing natural disasters. The proposed model aims to maximize served load, which has been structured as a mixed integer linear programming (MILP) problem. The IEEE 34 bus standard test system is used to investigate the effectiveness of the proposed structure. The results of the study show that the proposed structure can increase the served load and the supply-sufficiently of the smart grid power system.**

Keywords—Disaster, Demand Response Programs, Energy Storage, Micro Grid, Partitioning.

NOMENCLATURE

Index

i	Index of load point.
t	Index of time.
s	Index of scenarios.
m, n	Index of gas load point.

Parameters

ω^D	Priority of load points.
P^D	Active load.
ε_{DR}	Penetration Rate of load curtailment in DR
LPF^E_{up}	Penetration Rate of load shifting up in DR.
LPF^E_{down}	Penetration Rate of load shifting down in DR.
$\eta^E_{dis}, \eta^E_{ch}$	Discharge and charge efficiency.
ϑ^E_{loss}	Rate of energy loss in energy storage
P^E_{CAPA}	Capacity of storage
$P^E_{ch\_max}$	Maximum charge rate of Storage
$P^E_{dis\_max}$	Maximum discharge rate of Storage
$P^{DG,max}$	Maximum of active power DG capacity
$Q^{DG,max}$	Maximum of reactive power DG capacity
P_l^{max}, Q_l^{max}	Maximum of active and reactive line capacity
R, X	Resistance and inductance
k_c	Pipeline resistance coefficients
Γ	gas consumption rate

Variables

ρ	Binary variable of load status
DR^{LC}	Load curtailment
P^E_{down}, P^E_{up}	Upward and downward power of DR
I^E_{up}, I^E_{down}	Binary variable of upward and downward DR
$P^E_s(t,s)$	SOC of Storage
P^E_{ch}, P^E_{dis}	Charge and discharge of Storage

978-1-6654-3597-0/21/$31.00 ©2021 IEEE

I^E_{dis}, I^E_{ch}	Binary variable of charge and discharge
P, Q	Active and reactive output power of DG
u^{DG}	Binary variable of DG
$u(k)$	Binary variable of lines
V	Voltage of bus
f	The gas flow
ρ	The gas pressure
P_{input}	Input Gas
$P_{gas_{gen}}$	Gas consumption of DG

I. Introduction

Nowadays, the smart distribution system has been raised as the best platform for novel tools such as demand response programs (DRPs) and Energy Storages (ESs) [1]. The DRPs and ESs have a significant role in the smart grid disaster management problem [2]. In this regard, the role of emergency DRPs in increasing served load and decreasing outage time is undeniable. From customers' point of view, the reliability of continuous power supply is an important issue that affects their satisfaction level [3].

Hence, the operation of the smart grid in disaster time can be contemplated as a crucial challenge. Several works [4]–[7] have concentrated on distribution reconfiguration to decline the natural disaster impacts and handle this issue. In [8], the service restoration problem model is presented in order to maximize the served load. Two different management approaches including centralized and decentralized approaches, are modeled. The results of the study show that the centralized approach has a significantly higher cost than the decentralized approach.

Moreover, besides worldwide penetration of Distributed Generations (DGs) resources, challenges of operation and planning of distribution system have been altered. Referring to IEEE Std 1547.4, the smart distribution system can be partitioned into several microgrids to improve the reliability of the smart distribution system. In [9], a methodology has been provided to partition the conventional distribution system into supply-sufficient microgrids in the presence of ESs and DGs.

In [10], a two-stage partitioning method is proposed considering electrical energy vehicles, ES, and photovoltaic systems in the smart grid platform. The two-level optimization problem grid portioning has been performed in [11] with the simultaneous objective of served load maximization and loss minimization, where a novel power self-sufficiency index has been considered.

The smart distribution system partitioning has a positive effect on the operational risk decrement [12]. The grid portioning has been performed with the simultaneous aim of served load and confidence level maximization, while a novel power self-sufficiency index has been proposed. In [13], a risk management framework for island partitioning of smart radial distribution systems with DGs has been provided. The mentioned methods partition the system into prespecified fixed microgrids and can't work flexibly.

Moreover, the gas network infrastructure plays an important role in the distribution system due to the presence of gas turbine generators as the most popular DGs in the smart grid. In this regard, the gas network infrastructure is considered in recent smart microgrid studies. In [14] and [15], the gas pipeline infrastructure is modeled in the smart energy hub system. The failure occurrence in the gas pipelines maybe affects the performance of the power distribution system. On the other hand, some natural disasters (such as floods and earthquakes) can disrupt the gas network. Regarding the previous works, the lack of scrutinizing gas network impacts on smart grid partitioning is still a challenging issue to be investigated. Overall, considering the smart and flexible partitioning of the current distribution system can effectively increase the served load and the satisfaction rate of customers.

Therefore, in this paper, a novel flexible model for smart distribution system partitioning is presented, concentrating on served load maximization in the presence of DRPs and ESs. In the proposed model, the impacts of load priority are also considered. Moreover, to obtain more realistic results, the gas network constraints and electricity constraints are also contemplated. The model is structured in a GAMS (General Algebraic Modeling System) environment, and CPLEX is utilized to solve the proposed mixed-integer linear programming (MILP) problem. The remainder of this paper is organized as follows. The formulation of the proposed model is provided in section II. Section III presents the results of the case study. The conclusion is provided in Section IV.

II. Formulation of the Proposed Model

In this section, the formulation of the grid partitioning problem incorporating DRPs ESs and DGs has been provided. In this respect, the objective function of the problem is presented as (1):

$$Max \sum_{i=1}^{N_i} \sum_{t=1}^{N_t} \omega^D(i) \left(\rho(i,t) P^D(i,t) - DR^{LC}(i,t)\right) \quad (1)$$

The primary target of (1) is to maximize the distribution system serving load. $\omega^D(i)$ and $P^D(i,t)$ denote the load priority and active demand in i^{th} bus of the distribution system. Moreover, $\rho(i,t)$ is a binary variable that shows the on/off status of the demand. Here, the load curtailment variable is symbolized by $DR^{LC}(i,t)$. DRPs limitations are formulated by (2)-(6) in the grid partitioning problem.

$$DR^{LC}(i,t) \le \rho(i,t) \varepsilon_{DR} P^D(i,t) \quad (2)$$

$$\sum_{t=1}^{N_t} P^E_{down}(i,t) = \sum_{t=1}^{N_t} P^E_{up}(i,t) \quad (3)$$

$$0 \le P^E_{up}(t,i) \le LPF^E_{up} P^D(i,t) I^E_{up}(t,i) \quad (4)$$

$$0 \le P^E_{down}(t,i) \le LPF^E_{down} P^D(i,t) I^E_{down}(t,i) \quad (5)$$

$$0 \le I^E_{down}(t,i) + I^E_{up}(t,i) \le 1 \quad (6)$$

where (2) states that the hourly load curtailment should be lower than the prespecified percentage of hourly active load (ε_{DR}); (3) shows that the upward ($P^E_{up}(i,t)$) and downward ($P^E_{down}(i,t)$) active load per bus should be equal at the end of the scheduling time; (4) and (5) stand for upward and downward limits in load shifting DRPs, and (6) force to select one strategy (upward and downward DR).

LPF_{up}^{E} and LPF_{down}^{E} are the maximum percentage load in a time interval *t* and connection point *i* that the system operator can modify, respectively. Moreover, the upward and downward binary variables are represented by $I_{down}^{E}(t,i)$ and $I_{up}^{E}(t,i)$, respectively.

ESs restrictions are formulated via (7)-(12) in the grid partitioning problem. Constraint (7) shows an ES state of charge in a time; (8) stands for the electrical loss of the ES; the ES state of charge is restricted by (9); (10) and (11) stands for the charge and discharge bounds of ES, and (12) forces to select one strategy for ES; i.e., either charge or discharge.

The index *s* in (7)-(12) shows the ESs indices. Furthermore, the variable $P_{s}^{E}(t,s)$ indicates the state of charge of each ES (s) and time interval. Moreover, the $P_{ch}^{E}(t,s)$ and $P_{dis}^{E}(t,s)$ are the charge and discharge power of energy storage, respectively. The charge and discharge efficiency has been shown by η_{ch}^{E} and η_{dis}^{E} Respectively. Furthermore, the $P_{loss}^{E}(t,s)$ and ϑ_{loss}^{E} show the electrical loss of ESs and predefined percentage of the state of charge, respectively. The ESs capacity, maximum allowed charge, and discharge of energy storage are shown by parameters P_{CAPA}^{E}, $P_{ch\_max}^{E}$ and $P_{dis\_max}^{E}$.

$$P_{s}^{E}(t,s) = P_{s}^{E}(t-1,s) + P_{ch}^{E}(t,s)\eta_{ch}^{E} - P_{dis}^{E}(t,s)/\eta_{dis}^{E} - P_{loss}^{E}(t,s) \quad (7)$$

$$P_{loss}^{E}(t,s) = \vartheta_{loss}^{E} P_{s}^{E}(t,s) \quad (8)$$

$$0 \le P_{s}^{E}(t,s) \le P_{CAPA}^{E} \quad (9)$$

$$0 \le P_{ch}^{E}(t,s) \le P_{ch\_max}^{E} I_{ch}^{E}(t,s) \quad (10)$$

$$0 \le P_{dis}^{E}(t,s) \le P_{dis\_max}^{E} I_{dis}^{E}(t,s) \quad (11)$$

$$0 \le I_{dis}^{E}(t,s) + I_{ch}^{E}(t,s) \le 1 \quad (12)$$

The active and reactive power balance of smart distribution system are shown as follow:

$$\sum_{\forall k\in(i,0)} P(k,t) + \sum_{DG} P(DG,t) = \sum_{\forall k\in(0,i)} P(k,t) + \rho(i,t)P^{D}(i,t) - DR^{LC}(i,t) + \sum_{s=1}^{N_s}\left(P_{ch}^{E}(t,s) - P_{dis}^{E}(t,s)\right) - P_{up}^{E}(i,t) + P_{down}^{E}(i,t) \quad (13)$$

$$\sum_{\forall k\in(i,0)} Q(k,t) + \sum_{DG} Q(DG,t) = \sum_{\forall k\in(0,i)} Q(k,t) + \rho(i,t)Q^{D}(i,t) \quad (14)$$

The index *k* in (13) and (14) show the line number indices. The active and reactive power flow of lines are illustrated by $P(k,t)$ and $Q(k,t)$ variables, respectively.

The active and reactive generation power of DGs are limited as (15) and (16):

$$0 \le P(DG,t) \le P^{DG,max} u^{DG}(DG,t) \quad (15)$$

$$0 \le Q(DG,t) \le Q^{DG,max} u^{DG}(DG,t) \quad (16)$$

The binary variable $u^{DG}(DG,t)$ shows the on/off status of DG. Moreover, the maximum allowable generation active and reactive power are shown by parameter $P^{DG,max}$ and $Q^{DG,max}$ respectively.

The active and reactive power flow of lines are limited to maximum allowable active (P_{l}^{max}) and reactive (Q_{l}^{max}) rates as (17) and (18) respectively:

$$-u(k)P_{l}^{max} \le P(k,t) \le u(k)P_{l}^{max} \quad (17)$$

$$-u(k)Q_{l}^{max} \le Q(k,t) \le u(k)Q_{l}^{max} \quad (18)$$

Furthermore, (19) relates the voltage of each load point to the active and reactive power flow of each line. Moreover, (20) shows that the voltage of each load point is limited to a maximum and minimum level.

$$-\big(1-u(k)\big)M \le V(j,t) - V(i,t) - \frac{R(k)P(k,t)+X(k)Q(k,t)}{V_{ref}} \le \big(1-u(k)\big)M \quad (19)$$

$$0.95 \le V(i,t) \le 1.05 \quad (20)$$

The variable $u(k)$ indicates the on/off status of each power line. Furthermore, the ac power flow equations are relaxed by the big *M* method.

Furthermore, (21)-(27) indicate the gas flow equation in the smart microgrid. Equation (21) shows the relationship between gas pressure and gas flow in the gas pipelines. It should be noted that (21) is a non-linear equation. Therefore, (21) is linearized by considering the initial amounts of gas node pressures as (22). Equations (23) and (24) compare the gas pressures in the gas nodes ($m \ge n$). Equation (25) shows the gas node balance in the smart microgrids. Also, (27) shows the fuel amount of gas-fired DGs.

$$f(m,n,t) = k_{c}(m,n)\sqrt{\rho(m,t)^2 - \rho(n,t)^2} \quad (21)$$

$$f(m,n,t) = k_{c}(m,n)\frac{\big(\rho(m,t)\hat{\rho}(m,t) - \rho(n,t)\hat{\rho}(n,t)\big)}{\sqrt{|\hat{\rho}(m,t)^2 - \hat{\rho}(n,t)^2|}} \quad (22)$$

$$\rho(m,t) \ge \rho(n,t) \quad (23)$$

$$\rho(n,t) \ge \gamma\rho(m,t) \quad (24)$$

$$P_{input}(m,t) - \sum_{n} f(m,n,t) = P_{gas_{gen}}(m,t) \quad (25)$$

$$P_{gas_{gen}}(m,t) = \Gamma\, P^{DG}(i,t) \quad (26)$$

The variables $f(m,n,t)$ and $\rho(m,t)$ are the amount of gas flow and gas pressure, respectively. Also, the parameter $k_{c}(m,n)$ is the pipeline resistance coefficients vector, and it depends on the pipe diameter. Furthermore, Γ is the parameter of the gas consumption rate of DGs.

III. Numerical Study

A. Case study: IEEE 34 Bus test system

In this section, the numerical study has been performed on the verified IEEE 34 test system, as shown in Fig. 1. Table 1 shows the information of DGs. Moreover, the remained essential data of the proposed model has been provided in Table 2. The priority list of load points is presented in Table 3. It can be seen in Table 3 that the load points have been valued in 3 three different clusters, i.e. 0.5, 0.75, and 1.

Table. 1. DGs Information

	Active capacity (kW)	Reactive capacity (kVAR)
DG 1	240	120
DG 2	240	120
DG 3	240	120
DG 4	240	120

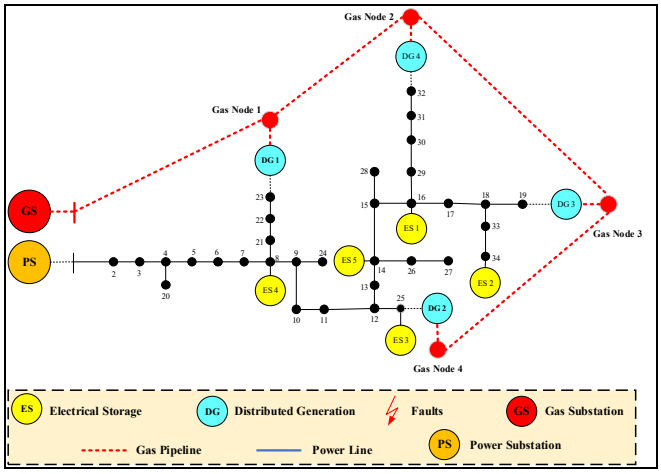

Fig.1. The Modified IEEE 34 bus test System

Table. 2. Parameter of the proposed model

Parameter	Amount	Parameter	Amount
ε_{DR}	0.2	γ	0.8
LPF_{up}^{E}	0.2	Γ	1.2
LPF_{down}^{E}	0.2	$P_{dis\ max}^{E}$	240
η_{ch}^{E}	0.9	$k_c(m,n)$	300
η_{dis}^{E}	0.9	$P_{ch\ max}^{E}$	240
ϑ_{loss}^{E}	0.95	P_{CAPA}^{E}	600 kW

Table. 3. Load priority list

Bus	Priority	Bus	Priority
1	0.5	18	0.5
2	0.5	19	0.75
3	0.5	20	0.5
4	0.75	21	1
5	1	22	0.75
6	0.5	23	1
7	0.75	24	1
8	0.5	25	1
9	1	26	0.5
10	0.75	27	1
11	1	28	0.5
12	0.5	29	1
13	0.75	30	0.5
14	1	31	0.75
15	0.5	32	1
16	0.75	33	0.5
17	1	34	1

It should be noted that the base value of power in the IEEE 34 bus test system is equal to 12 MVA. Additional inputs to IEEE 34 bus test system are adopted from [17]. Fig. 2 and 3 show the active and reactive load of the modified IEEE 34 bus test system, respectively. In order to investigate the effects of disaster on the smart grid, two different types of faults have been investigated:

• A fault in the electrical structure considered in the power line between electrical nodes 1 and 2.

• A fault in the gas structure is considered in gas nodes 2 and 3.

In each fault case, four scenarios are investigated to evaluate the effects of DRPs and ESs on the smart microgrids served load percentage. Table 4 shows the considered scenarios of the proposed model.

Table. 4. Scenario Description

	DRPs	ESs
S 1	-	-
S 2	✓	-
S 3	-	✓
S 4	✓	✓

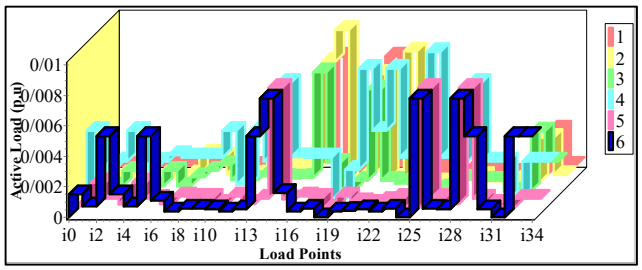

Fig. 2. The active load of the smart distribution system

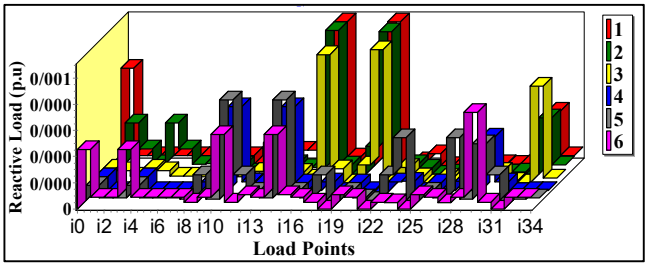

Fig. 3. The reactive load of the smart distribution system

B. *Results of Case 1 (Fault in electrical lines)*

In this case, the fault occurs in the electrical infrastructure in the power line between buses 1&2. Also, it is obvious that this bus is a critical point of the distribution system.

Fig. 4 shows the location of the fault point and the output of the proposed partitioning method. The results show that the conventional distribution system has been partitioned into three self-sufficient partitions. In this respect, the connections between buses 8-21 and buses 12-13 are disconnected.

Moreover, Table 5 shows the served load of the smart microgrids after the fault occurred. In the first scenario, the served load is equal to % 90 of the total load, and it is significantly lower than other scenarios since the DRPs and ESs are neglected.

Furthermore, considering DRPs and ESs in the disaster time has been caused to increase in the served load. The results presented in Table. 5 show that the effectiveness of DRPs is higher than ESs in the smart microgrid served load. This is reasonable since DRPs are distributed over the microgrid and hence logically outperform the centralized ESs.

Fig. 5 shows the SOC of ESs in the smart microgrids in each time interval. Referring to Fig. 2 and Fig. 3, it can be concluded that the active and reactive load in time intervals 4 and 6 are higher than other time intervals.

Consequently, ESs tend to discharge in peak intervals. Moreover, DRPs are another alternative to increase the served load of microgrids.

Fig. 6 shows the application of the DRPs in the microgrids. The results show that the demands in time intervals 4 and 6 are shifted down in most load points.

Table. 5. Served load in each scenario of case 1

Scenario	Served Load (%)
S 1	90.10
S 2	96.57
S 3	93.03
S 4	98.53

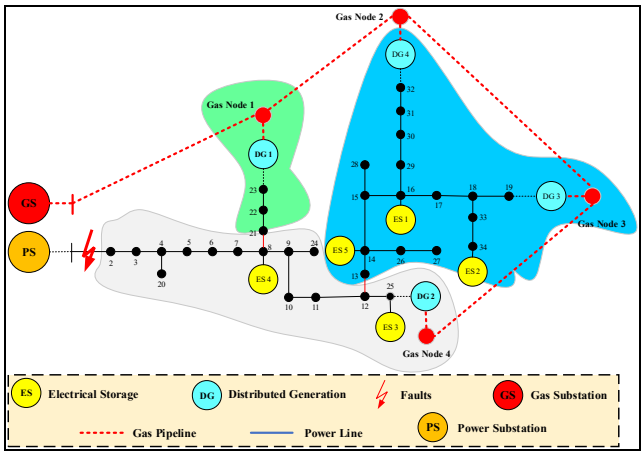

Fig. 4. The distribution partitioning into self-sufficient partitions in case 1

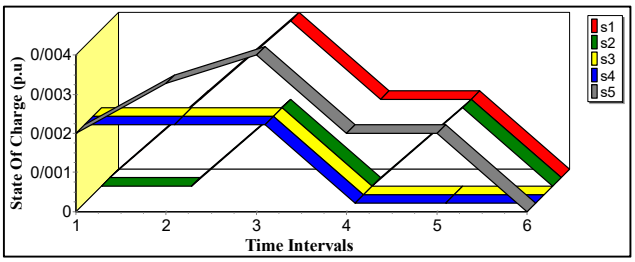

Fig. 5. The energy storage status in case 1

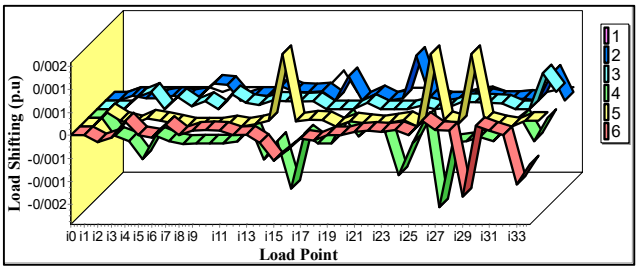

Fig. 6. The load shifting in case 1

C. *Results of Case 1 (Fault in the gas pipeline)*

In this case, the fault occurs in the gas pipeline between gas nodes 3 and 4. Therefore, the fuel of DG 2 is not satisfied and it is out of service forcibly. Fig. 6 shows the fault location and occurred partitions by the proposed model. The results show that the line between 11 and 12 has been disconnected and two separate microgrids have been formed.

Table. 6 shows the served load of microgrids in case 2. Also similar to Table. 2, the DRPs have a higher effect on served load than ESs. One of the important reasons for this issue is that the DRPs are scattered in all load points. Referring to the line limits of the distribution system, the performance of DRPs is higher than ESs. Also, Fig. 7 shows the SOC of ESs in the smart energy system. Furthermore, Fig. 8 shows the optimal amount of DRPs in the smart microgrid. Similar to Case 1, the load shifting and ESs operation are caused to linearize the demand pattern.

Table. 6. Served load in each scenario of case 2

Scenario	Served Load (%)
S 1	90.66
S 2	94.74
S 3	94.162
S 4	99.169

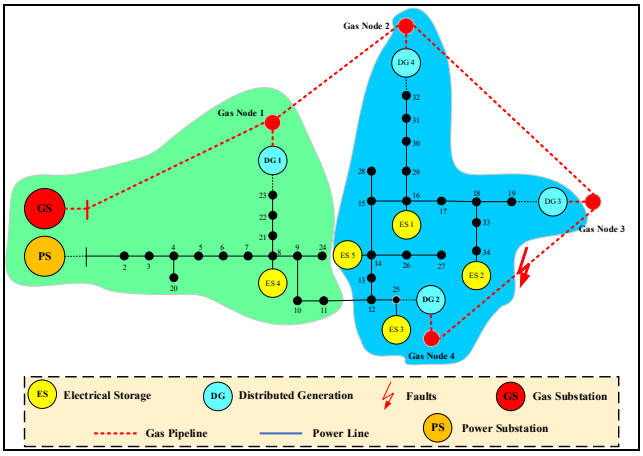

Fig. 6. The distribution partitioning into self-sufficient partitions in case 2

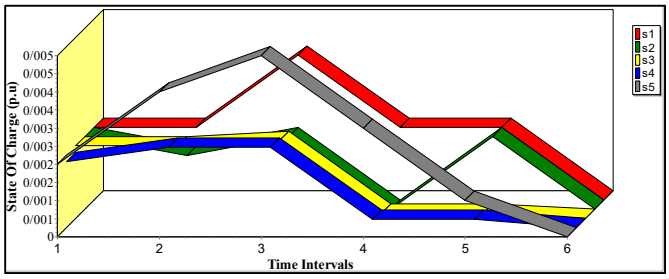

Fig. 7. The energy storage status in case 2

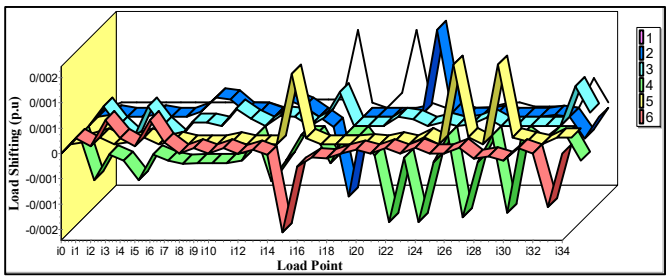

Fig. 8. The load shifting in case 2

IV. Conclusion

In this paper, a novel flexible partitioning method was proposed. The results of the study show that the location and type of faults determine the form of partitions in the smart microgrids. DRPs and ESs have a very important role in the served load increment. The served load increment effect of DRPs (load curtailment and load shifting programs) is higher than ESs. Moreover, smart microgrid resources flexibility plays an important role in smart microgrids disaster management. Also, DGs strategic location can help the proposed problem by participating in the smart microgrids self-healing phase. Furthermore, the case study results analysis and the comparison of considered scenarios show that the proposed method can significantly increase the self-sufficiency and served load of the smart microgrid. The effects of load uncertainty and the unpredictable production of renewable DGs in the smart microgrid partitioning problem will be studied in future works.

References

[1] S. Dorahaki, M. Rashidinejad, A. Abdollahi, and M. Mollahassani-pour, "A novel two-stage structure for coordination of energy efficiency and demand response in the smart grid environment," Int. J. Electr. Power Energy Syst., vol. 97, pp. 353–362, 2018.

[2] S. Dorahaki, R. Dashti, and H. R. Shaker, "Optimal energy management in the smart microgrid considering the electrical energy storage system and the demand-side energy efficiency program," J. Energy Storage, vol. 28, Apr. 2020.
[3] S. Dorahaki, M. Rashidinejad, M. Mollahassani-pour, and A. Bakhshai, "An efficient hybrid structure to solve economic-environmental energy scheduling integrated with demand side management programs," Electr. Eng., vol. 101, no. 4, pp. 1249–1260, Dec. 2019.
[4] T. Ding, Y. Lin, Z. Bie, and C. Chen, "A resilient microgrid formation strategy for load restoration considering master-slave distributed generators and topology reconfiguration," Appl. Energy, vol. 199, pp. 205–216, Aug. 2017.
[5] M. I. Pathan, M. Al-Muhaini, and S. Z. Djokic, "Optimal reconfiguration and supply restoration of distribution networks with hybrid microgrids," Electr. Power Syst. Res., vol. 187, p. 106458, Oct. 2020.
[6] S. S. Fazlhashemi, M. Sedighizadeh, and M. E. Khodayar, "Day-ahead energy management and feeder reconfiguration for microgrids with CCHP and energy storage systems," J. Energy Storage, vol. 29, p. 101301, Jun. 2020.
[7] J. J. Marquez, A. Zafra-Cabeza, C. Bordons, and M. A. Ridao, "A fault detection and reconfiguration approach for MPC-based energy management in an experimental microgrid," Control Eng. Pract., vol. 107, p. 104695, Feb. 2021.
[8] A. Arif and Z. Wang, "Networked microgrids for service restoration in resilient distribution systems," IET Gener. Transm. Distrib., vol. 11, no. 14, pp. 3612–3619, Sep. 2017.
[9] M. Barani, J. Aghaei, M. A. Akbari, T. Niknam, H. Farahmand, and M. Korpas, "Optimal Partitioning of Smart Distribution Systems Into Supply-Sufficient Microgrids," IEEE Trans. Smart Grid, vol. 10, no. 3, pp. 2523–2533, May 2019.
[10] J. Zhu, W. Gu, P. Jiang, Z. Wu, X. Yuan, and Y. Nie, "Integrated approach for optimal island partition and power dispatch," J. Mod. Power Syst. Clean Energy, vol. 6, no. 3, pp. 449–462, May 2018.
[11] Z. Wang and J. Wang, "Self-Healing Resilient Distribution Systems Based on Sectionalization Into Microgrids," IEEE Trans. Power Syst., vol. 30, no. 6, pp. 3139–3149, Nov. 2015.
[12] Z. Jingxiang, N. Huanna, and Z. Xiaoxue, "Island partition of distribution network with microgrid based on the energy at risk," IET Gener. Transm. Distrib., vol. 11, no. 4, pp. 830–837, Mar. 2017.
[13] Z. N. Popovic, S. D. Knezevic, and B. S. Brbaklic, "A Risk Management Procedure for Island Partitioning of Automated Radial Distribution Networks With Distributed Generators," IEEE Trans. Power Syst., vol. 35, no. 5, pp. 3895–3905, Sep. 2020.
[14] S. Dorahaki, A. Abdollahi, M. Rashidinejad, and M. Moghbeli, "The role of energy storage and demand response as energy democracy policies in the energy productivity of hybrid hub system considering social inconvenience cost," J. Energy Storage, p. 102022, Oct. 2020.
[15] A. Ghanbari, H. Karimi, and S. Jadid, "Optimal planning and operation of multi-carrier networked microgrids considering multi-energy hubs in distribution networks," Energy, vol. 204, p. 117936, Aug. 2020.